Journal of Cell Science 104, 861-872 (1993)
Printed in Great Britain © The Company of Biologists Limited 1993

Inhibition of protein kinases by 6-dimethylaminopurine accelerates the transition to interphase in activated mouse oocytes

Maria S. Szöllösi[1,*], Jacek Z. Kubiak[2], Pascale Debey[3], Henri de Pennart[2], Daniel Szöllösi[1] and Bernard Maro[2]

[1]INRA, Unité de Biologie de la Fécondation, Station de Physiologie Animale, F-78352 Jouy-en-Josas Cédex, France
[2]Laboratoire de Physiologie du Développement, Institut Jacques Monod, CNRS-Université Paris VII, F-75005 Paris, France
[3]Unité de Développement concertée INSERM-INRA U 310, Institut de Biologie Physico-Chimique, 13 rue Pierre et Marie Curie, F-75005 Paris, France

*Author for correspondence

SUMMARY

Mouse oocyte activation is followed by a peculiar period during which the interphase network of microtubules does not form and the chromosomes remain condensed despite the inactivation of MPF. To evaluate the role of protein phosphorylation during this period, we studied the effects of the protein kinase inhibitor 6-dimethylaminopurine (6-DMAP) on fertilization and/or parthenogenetic activation of metaphase II-arrested mouse oocytes. 6-DMAP by itself does not induce the inactivation of histone H1 kinase in metaphase II-arrested oocytes, and does not influence the dynamics of histone H1 kinase inactivation during oocyte activation. However, 6-DMAP inhibits protein phosphorylation after oocyte activation. In addition, the phosphorylated form of some proteins disappear earlier in oocytes activated in the presence of 6-DMAP than in the activated control oocytes. This is correlated with the acceleration of some post-fertilization morphological events, such as sperm chromatin decondensation and its transient recondensation, formation of the interphase network of microtubules and pronuclear formation. In addition, numerous abnormalities could be observed: (1) the spindle rotation and polar body extrusion are inhibited; (2) the exchange of protamines into histones seems to be impaired, as judged by the morphology of DNA fibrils by electron microscopy; (3) the formation of a new nuclear envelope around the sperm chromatin proceeds prematurely, while recondensation is not yet completed. These observations suggest that the 6-DMAP-sensitive kinase(s) is (are) involved in the control of post-fertilization events such as the formation of the interphase network of microtubules, the remodelling of sperm chromatin and pronucleus formation.

Key words: 6-DMAP, chromatin, mouse oocytes, sperm, histone kinase, fertilization, parthenogenetic activation, phosphorylation

INTRODUCTION

Activation of the mouse oocyte is a complex process during which the oocyte passes from meiotic control of the cell cycle to mitotic control. The oocyte, previously arrested at the second meiotic metaphase (M II), extrudes the second polar body and enters a very peculiar period, characterized by the delay of some morphological events when compared to the embryonic mitotic transition from M-phase to interphase. In this period, the oocyte chromatin remains condensed and the interphase network of microtubules is not formed until at least one hour after the second polar body extrusion (M. Weber, J. Z. Kubiak and B. Maro, unpublished), despite maturation-promoting factor (MPF) inactivation (Weber et al., 1991). During the 3-to-4 h following activation, the sperm nucleus is remodelled completely, including the replacement of protamines by histones (Kopečný and Pavlok, 1975a; Kopečný and Pavlok, 1975b; Nonchev and Tsanev, 1990; Rodman et al., 1981). The condensed oocyte chromatin remains in the "telophase" state while the sperm chromatin decondenses, and then undergoes a transient recondensation (Adenot et al., 1991). This recondensed state of the male chromatin corresponds to the beginning of the formation of the male pronucleus, which occurs later than the formation of the female pronucleus. Both sets of chromatin then decondense almost synchronously. The mechanisms involved in the control of this long "telophase" state are not known.

When compared to interphase, M-phase is characterized by a high level of protein phosphorylation, due to the activity of many kinases activated by MPF. In the mouse oocyte, at the time of extrusion of the second polar body, the activity of MPF drops rapidly (Choi et al., 1991; Weber et al., 1991). The pattern of protein synthesis also changes after activation, mainly because of post-translational modifications (phosphorylation) of at least three groups of proteins:

30, 35 and 45 kDa (Howlett, 1986; Howlett and Bolton, 1985). All of these changes take place more slowly during entry into the first interphase, in contrast to the subsequent mitotic divisions, where they are rapid (Howlett, 1986). The 35 kDa protein complex remains phosphorylated for up to 4 h after sperm penetration. Moreover, the newly synthesized 35 kDa proteins become actively phosphorylated during this period, in contrast to the 30 kDa and 45 kDa polypeptides. Thus, the release from M II arrest is not characterized by a rapid and massive dephosphorylation but rather, by a slow and progressive inactivation of some protein kinases and activation of protein phosphatases.

We used the non-specific inhibitor of protein kinases, 6-dimethylaminopurine (6-DMAP; Néant and Guerrier, 1988) during the fertilization or parthenogenetic activation and subsequent culture of mouse oocytes to interfere with the normal course of protein phosphorylation during entry into the first interphase. We show that 6-DMAP is not able to induce MPF inactivation in M II-arrested oocytes, nor does it modify the kinetics of MPF inactivation after oocyte activation. However, following oocyte activation, 6-DMAP inhibits the phosphorylation of the 35 kDa complex, thus accelerating the disappearance of the phosphorylated form of these proteins. This is accompanied by the acceleration of morphological events, like oocyte chromosome decondensation, decondensation and recondensation of the sperm chromatin, pronucleus formation and formation of the interphase microtubule network.

MATERIALS AND METHODS

Oocytes

Ovulated oocytes were collected from 9-11-week-old female mice from the OF1 or Swiss strains. Ovulation was induced by intraperitoneal injections of 5 i.u. of pregnant mare's serum gonadotrophin (PMSG) and human chorionic gonadotrophin (hCG), 48 h apart. Oocytes were collected 16-17 h post-hCG in medium 2 (M2; Quinn et al., 1982). The follicle cells were removed with hyaluronidase (300 i.u./ml in M2). For in vitro fertilization, the zona pellucida was removed with α-chymotrypsin (30 μg/ml in M2) or with acid Tyrode's solution (Nicolson et al., 1975).

Parthenogenetic activation and fertilization

Oocytes with zonae pellucidae were activated by a 6 min exposure to 8% ethanol solution in M2 + BSA medium (Cuthberson, 1983). Spermatozoa collected from the caudae epididymides of an adult F_1 (C57BL × CBA) male were capacitated for 1 h in 1 ml of Whittingham's M16 medium modified by Fraser and Drury (1975), containing 32 mg/ml crystalline BSA (Sigma) and equilibrated for 24 h at 37.5°C in an atmosphere of 5% CO_2 in air under liquid paraffin. Zona-free oocytes were inseminated for 10-15 min in fertilization medium containing approximately 1×10^6 sperm/ml, carefully washed and cultured in M2 + BSA.

Observation of live oocytes and zygotes

Oocytes were labelled for 30 min with 5 ng/ml Hoechst 33342 in M2 + BSA, or M2 + BSA containing 6-DMAP, before activation or fertilization. For observation, they were individually distributed in small droplets of culture medium under liquid paraffin in specially prepared Petri dishes (for technical details see Debey et al., 1989). Eggs were observed at different times after activation or fertilization. Hoechst was removed carefully by washing after every observation and added again 0.5 h before the following observation. In the case of fertilization, the rapid motion of spermatozoa attached to the oocyte surface rendered observation of the chromatin in living oocytes impossible. Zygotes were therefore collected at selected times and fixed in EM fixative containing Hoechst. Observations were made with a Nikon (Diaphot) inverted microscope equipped with a 100 W mercury lamp (Osram HBO) and a thermostated box, connected to an intensified camera (Lhesa) and an image processing system (Quantel Sapphire; Debey et al., 1989). Chromatin surface in the focal plane was measured using an image analysis program (Quantel). The chromatin outline was defined either by thresholding the fluorescence intensity, or by manual drawing.

Electron microscopy

Oocytes and zygotes were fixed in a solution containing 2.5% glutaraldehyde, 0.7% paraformaldehyde in 0.075 M phosphate buffer, pH 7.2-7.4, containing 0.2-0.5% potassium ferricyanide (Yotsuyanagi and Szöllösi, 1981). They were washed in the same buffer and post-osmicated in 2% OsO_4 in distilled water, washed three times in distilled water and stained overnight in toto in 0.5% aqueous uranyl acetate solution. They were then dehydrated in a series of increasing concentrations of ethanol solutions and embedded in Epon. Thin sections were stained with uranyl acetate and lead citrate.

Oocyte fixation and immunocytochemical staining

Zona-free oocytes were placed in specially designed glass or stainless steel chambers, as described by Maro et al. (1984), except that the chambers were coated with 0.1 mg/ml concanavalin A (Sigma). The samples were centrifuged at 450 ***g*** for 8-10 min at 37°C, and left for 10 min at 37°C after centrifugation. They were then fixed as described in de Pennart et al. (1988) with 0.1% glutaraldehyde (Sigma) in PBS supplemented with 1% Triton X-100 (Boehringer Mannheim GmbH). After a 5 min wash in PBS they were extracted with 2% Triton X-100 for 30 min, incubated in 10 mg/ml $NaBH_4$ in PBS (three incubations of 10 min each), washed twice in PBS and processed for immunofluorescence as described in Maro et al. (1984).

We used the rat monoclonal antibody YL1/2 specific for tyrosinated α-tubulin (Kilmartin et al., 1982) and a fluorescein-labelled, anti-rat antibody (Miles) second layer. The chromatin was visualized using propidium iodide (Molecular Probes; 5 μg/ml in PBS).

Photomicroscopy

The coverslips were removed from the chambers and samples were mounted in Citifluor (City University, London, UK) and viewed under a Leitz Diaplan microscope. Photographs were taken on Kodak T-max 400 film using a Leitz Orthomat photographic system. Confocal laser scanning microscopy was performed using a BioRad MRC-600, mounted on an Optiphot II Nikon microscope equipped with a 60× objective (plan apo; NA 1.4). For fluorescein, an argon ion laser adjusted to 488 nm wave length was used, close to the maximum of absorption of fluorescein, and for propidium iodide a helium-neon ion laser adjusted to 543 nm was used. The emitted light was separated by a dichroic mirror (540DF30), and a DR565 long pass filter was placed in front of the photomultiplier collecting the fluorescein emission and a EF600LP long pass filter in front of the photomultiplier collecting the propidium iodide emission. The adjustment of the confocal system allowed a field depth of about 0.6 μm. Double fluorescence images were acquired in two passes, fluorescein first and propidium iodide second, to avoid any bleeding from one chan-

nel into the other. When necessary, the emitted signal was digitized by "photon counting" in order to increase the signal-to-noise ratio and each section was scanned 30-to-50 times. Photographs were taken on Kodak T-max 100 film using a Nikon F-301 camera mounted on a high resolution monitor.

Histone H1 kinase assay

Histone H1 kinase activity was determined as described by Félix et al. (1989) in HK buffer (80 mM β-glycerophosphate, 20 mM EGTA, pH 7.3, 15 mM $MgCl_2$, 1 mM DTT, 1 mM PMSF, 10 μg/ml leupeptin, 10 μg/ml pepstatin, 10 μg/ml aprotinin), using exogenous histone H1 (H III-S from calf thymus, Sigma) as substrate. Samples, each containing 40 oocytes in 5 μl of water, were lysed by freezing and thawing three times, diluted twice in double concentrated HK buffer (2 × HK) and incubated for 15 min at 20°C in the presence of 3.3 mg/ml histone H1, 1 mM ATP and 0.25 mCi/ml [^{32}P]ATP. In order to study the effect of 6-DMAP on histone H1 kinase activity in vitro, the drug was added to the reaction tube at a final concentration of either 2.5 or 1.2 mM. The reaction was stopped by the addition of a similar volume of double concentrated sample buffer (Laemmli, 1970) and incubation for 2 min at 90°C. The samples were then electrophoresed on a 10% SDS-polyacrylamide gel (Laemmli, 1970). To test the specificity of the reaction, the $p34^{cdc2}$ kinase (histone H1 kinase) was removed by centrifugation from the control sample using $p13^{suc1}$-coated Sepharose beads. To calculate the relative percentages of activated oocytes, control groups were cultured for 5-6 h and scored for the presence of pronuclei. Alternatively, some samples were stained with Hoechst 33342 as described previously (Kubiak et al., 1991) and examined under the fluorescence microscope shortly after polar body extrusion.

Metabolic labelling

Oocytes were sampled in groups containing 40 oocytes and incubated in the labelling medium (M2 + BSA containing 500 μCi/ml ^{35}S-methionine or phosphate-free M2 + BSA containing 500 μCi/ml ^{32}P-orthophosphate) for 1 h starting at 0, 1, 2 and 3 h after activation. Oocytes were then washed in three large drops of M2 + BSA and collected in 5 μl double strength sample buffer for analysis by 10% SDS-PAGE (Laemmli, 1970). For pulse-chase experiments, approximately 500-800 M II oocytes were labelled for 1 h as described above, washed in medium containing non-radioactive methionine (or phosphate), and then cultured in M2 + BSA. They were activated as described above and sampled in groups of 40 oocytes at the time indicated.

Experimental variants

A6: oocytes were activated in the presence of 2.5 mM 6-DMAP and then cultured in the presence of the drug; 6A6: oocytes were cultured first in 2.5 mM 6-DMAP for 1 h and then activated and cultured in the presence of the drug; F6: oocytes were fertilized and cultured in the presence of 2.5 mM 6-DMAP. In addition, 0.6 mM and 1.2 mM 6-DMAP were used in certain experiments.

Controls

Oocytes were activated (A) or fertilized (F) and then cultured in M2 + BSA.

In every experimental and control group, Hoechst-stained oocytes were examined at 0.5, 1.0, 1.5, 3.0 and 4.5 h of culture. From each group observed, at least 3 specimens were studied by electron microscopy. In both experimental and control groups, only monospermic zygotes were taken for EM study.

The chromatin surface was measured in mono- and dispermic embryos because the development of both spermatozoa was comparable with the monospermic condition, as observed previously by Witkowska (1981).

RESULTS

Sequence of morphological events taking place after activation

The observations from living, parthenogenetically activated or fertilized oocytes stained with Hoechst showed that development was not synchronous and that the timing of development was not identical for both groups (Tables 1 and 2). Spindle rotation and polar body formation were observed earlier in fertilized than in artificially activated eggs. At the electron microscope level, during spindle rotation, we observed that one set of telophase female chromosomes remained in contact with a thick cortical actin layer (Fig. 6A), which was present also over the metaphase II spindle.

When we studied the changes in the organization of the microtubule network by immunofluorescence with an anti-tubulin antibody, we observed that an interphase network of microtubules started to form in control oocytes approximately 1 h after the beginning of the second polar body extrusion (i.e. 1.5-1.7 h after ethanol treatment; Weber, Kubiak and Maro, in preparation). Before this time, microtubules are not usually detected in the cytoplasm and the only microtubules present were found in the region of the midbody joining both sets of chromosomes (Fig. 2A-D).

The dense chromatin mass observed after telophase differed from telophase chromosomes in that it was round or oval, smaller than in telophase and heterogeneous in fluorescence (compare Fig. 1B and D). This dense chromatin mass was characterized by heterogeneous chromatin density and the presence of cytoplasmic vesicles attached to

Table 1. Development of female chromatin in eggs activated in the absence (A) or presence (A6 and 6A6) of 6-DMAP

Time (h) post-activation	Experimental variant (n)	Anaphase and telophase	Dense chromatin masses	Pronuclei
0.5	A (30)	100		
	A6 (23)	100		
	6A6 (20)		100	
1.0	A (53)	100		
	A6 (44)	34	66	
	6A6 (8)		60	40
1.5	A (88)	96	4	
	A6 (36)	16	8	86
	6A6 (12)		8	92
2.5	A (50)	49	20	31
	A6 (20)			100
	6A6 (12)			100
4.0	A (22)		32	68
	A6 (4)			100
	6A6 (12)			100
5.0	A (26)			100
	A6 (31)			100
	6A6 (20)			100

For each time point the number of eggs examined is given in brackets (*n*). Results are given as percentages.

Table 2. Development of female chromatin in eggs fertilized in the absence (F) or presence (F6) of 6-DMAP

Time (h) post-activation	Experimental variant (n)	Anaphase and telophase	Dense chromatin masses	Pronuclei
0.5	F (9)			
	F6 (15)	73		
1.0	F (15)	100		
	F6 (15)	60	13	27
1.5	F (19)	37	63	
	F6 (25)	48	28	24
2.0	F (14)		71	29
	F6 (31)			100
3.0	F (25)		64	36
	F6 (38)			100
4.5	F (14)			100
	F6 (30)			100

For each time point the number of eggs examined is given in brackets (n). Results are given as percentages.

the chromatin surface, indicating nuclear envelope formation (Fig. 1C). This stage was observed 1.5 h after fertilization but generally later in artificially activated oocytes (Tables 1 and 2). At the same time, in fertilized eggs, the sperm was decondensed in 50% of eggs and recondensed in the remaining 50% (Fig. 4A, B). 3h after fertilization, the chromatin from the sperm was recondensed in 64% of eggs and a male pronucleus with nucleoli was formed in the others. The measurement of chromatin surface demonstrated a phase of recondensation of the sperm chromatin during development (Fig. 3).

6-DMAP accelerates the formation of the interphase microtubule network

In the presence of 1.2 mM or 2.5 mM 6-DMAP, we observed large cytoplasmic microtubule asters as soon as anaphase II was completed (about 20 min after ethanol treatment). In addition, numerous long microtubules radiated from the vicinity of chromosomes. These microtubules rapidly formed the interphase network (Fig. 2E-H). At the lowest drug concentration tested (0.6 mM), the interphase microtubules appeared slightly later than at higher concentrations, but still sooner than in the controls.

6-DMAP accelerates the formation of pronuclei

Oocytes activated (parthenogenetically or by fertilization in vitro) in the presence of 6-DMAP and then cultured further in the presence of the drug, developed faster than the controls (Tables 1, 2; Fig. 3). One hour after activation, the female chromatin was already at the dense mass stage, with formation of a nuclear envelope. 1.5 h after activation, the first female pronuclei containing a few nucleoli, were already observed. When oocytes pretreated with 6-DMAP for 1h were activated in the presence of the drug, the events following activation were accelerated further (Table 1). 30 min after activation, one or two very close chromatin dense masses were observed (Fig. 4E) which usually formed a single big pronucleus later (Fig. 4F).

Decondensation and recondensation of the sperm nuclei in Hoechst-stained zygotes resembled controls, except that all phases were accelerated in the presence of 6-DMAP. Further as sperm nuclei remodelling was asynchronously accelerated, a decrease in the chromatin surface was not obvious in 6-DMAP-treated zygotes when the surface was

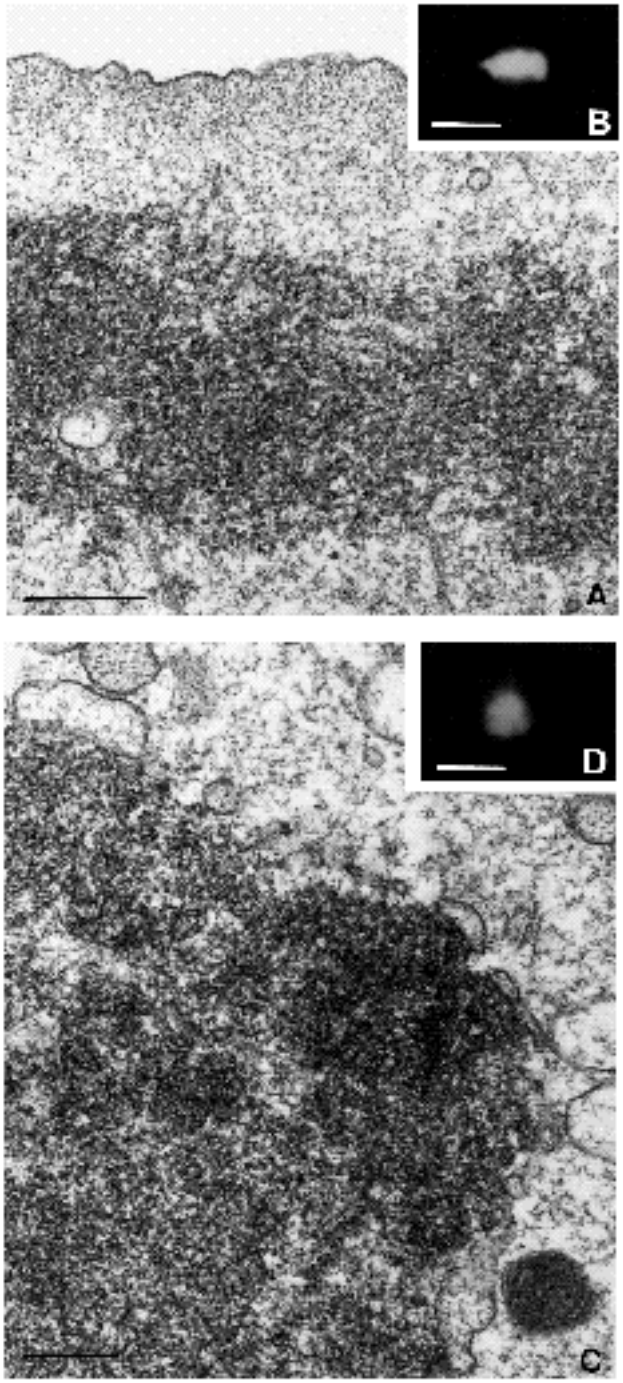

Fig. 1. Chromatin morphology in control oocytes as observed under the electron microscope (A, C) and the fluorescence microscope in vivo (B, D). Telophase chromatin (A, B) and dense chromatin mass (C, D). Note the layer of cortical microfilaments overlying the chromatin in A and the presence of membrane vesicles around the chromatin in C. Bars, 0.25 μm (A and C), 10 μm (B and D).

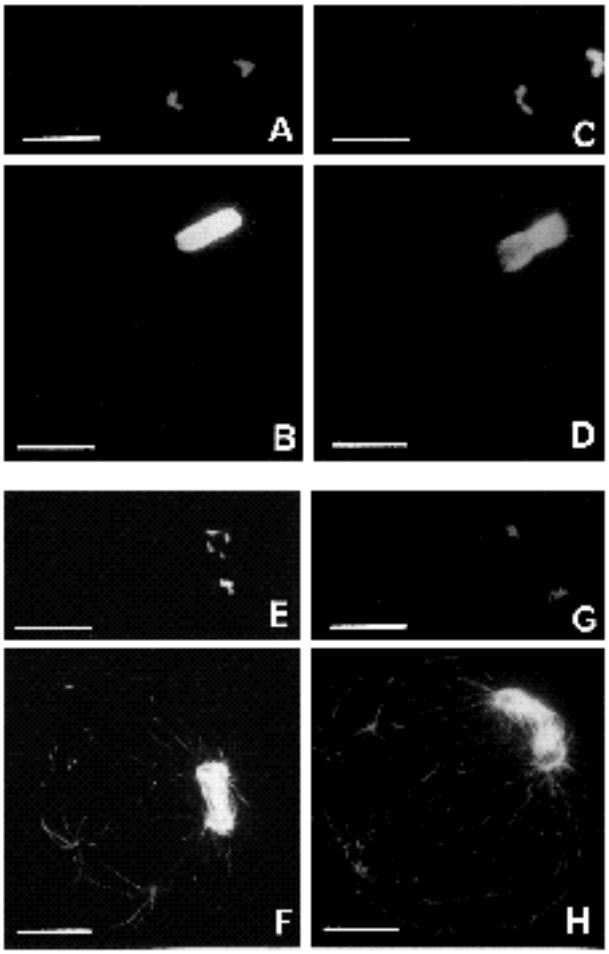

Fig. 2. Activated eggs double stained for chromatin (A, C, E, G) and tubulin (B, D, F, H). Bars, 20 μm. (A-D) Control eggs, 15 min (A, B) and 30 min (C, D) after polar body extrusion. Note that microtubules are only present in the midbody area joining the oocyte and the polar body. (E-H) Oocyte activated in 1.2 mM 6-DMAP 15 min (E, F) and 30 min (G, H) after the time of polar body extrusion in the control group. Note that large cytoplasmic microtubule asters are present in the cytoplasm and that long microtubules radiate from the vicinity of chromosomes.

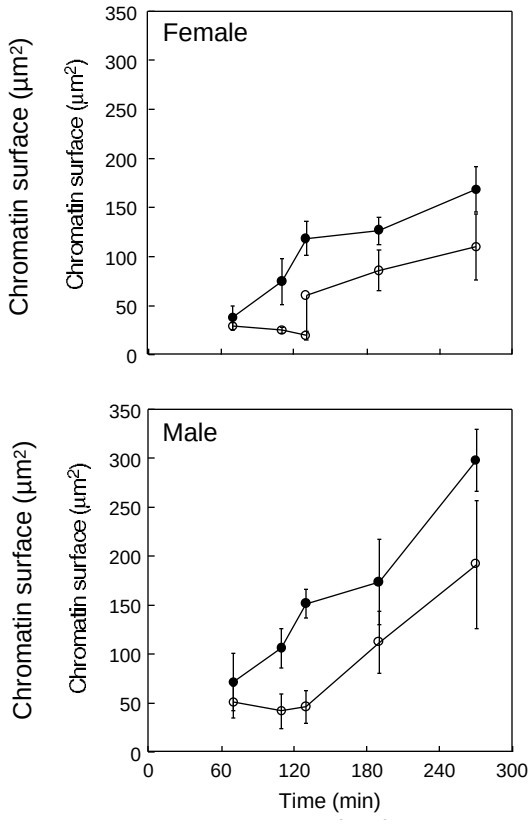

Fig. 3. Changes in the area of the largest section through the female (top panel) and male (bottom panel) chromatin in fertilized eggs. The number of chromatin areas measured varies between 10 and 27 for each time point and the results are given as the mean ± standard deviation. Time in minutes post-fertilization. (○) control; (●) 6-DMAP-treated.

measured as a function of time (Fig. 3). In some decondensed sperm heads, the Hoechst image showed more intensely fluorescing spots, which were bigger than those observed in the controls (Fig. 4D). The fertilization cones were not formed, and the male pronucleus had usually formed after 1.5 h of culture, much earlier than in the controls, and their growth was also faster (Table 2, Fig. 3).

6-DMAP induces abnormalities in pronuclear formation

The dense chromatin mass, corresponding to the forming female pronucleus, was often very irregular in shape and surrounded by cytoplasmic vesicles. When the oocyte was treated with 6-DMAP before activation, this mass usually occupied the entire space left by the spindle between two microtubule organizing centers (MTOCs). It looked rather like a group of aggregated chromosomes, enclosing many vesicles and annulate lamellae (Fig. 5A). The ultrastructure of the decondensed pronuclei found at later times was normal.

Electron microscopy showed abnormalities during remodelling of the sperm heads in oocytes exposed to 6-DMAP. In some sperm heads, the chromatin recondensation had already begun in some regions before chromatin decondensation had been completed in other regions. In such sperm heads, classified using Hoechst staining as decondensed, primarily condensed chromatin remained associated with the implantation fossa of the flagellum (Fig. 5B, C). The entire area of the decondensed chromatin was surrounded by vesicles originating from the spermatozoon nuclear envelope (Fig. 5D), that in control oocytes had disappeared very rapidly. Inside the decondensed chromatin, islands of more condensed chromatin were present, surrounded by vesicles with a few nuclear pores present between them (Fig. 5E). The presence of pores in this area suggests strongly the formation of a new nuclear envelope. The part of the old nuclear envelope from the spermatozoon (the redundant segment containing nuclear pores) was found in the same specimen on other serial sections (Fig. 5C). Within the decondensed chromatin, tightly packed straight or undulating bundles of chromatin filaments were present for a long time (Fig. 5D), while they disappeared earlier in controls. These bundles of filaments were still pre-

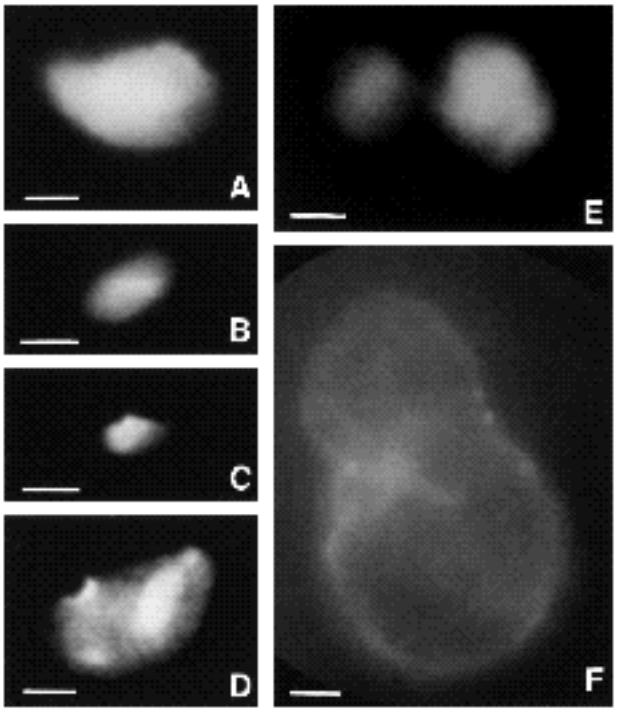

Fig. 4. Fluorescent images of chromatin in vivo. (A, B) In control eggs, 1.5 h after fertilization. The sperm is decondensed in 50% of eggs (A) and recondensed in the remaining 50% (B). (C) Condensed sperm head after penetration in a 6-DMAP treated egg. (D) Decondensed sperm head in a 6-DMAP treated egg. Note the intensely fluorescing spots. (E, F) Oocytes pretreated with 6-DMAP for 1 h and activated in the presence of the drug. Note the presence of 2 dense masses at 0.75 h (E) and of a single, large pronucleus at 5 h (F). Bars, 5 μm.

sent in some recondensed sperm chromatin in the presence of the drug (Fig. 5F). The incorporation cone was usually absent above the decondensed or recondensed sperm chromatin, but a thick actin layer was located along the inner surface of the plasma membrane. Finally, the ultrastructure of the male pronucleus formed in the presence of the drug did not differ from controls.

6-DMAP inhibits polar body formation

In 96.5% (136/141) of activated and 80% (68/85) of fertilized oocytes the second polar body was not extruded in the presence of 2.5 mM 6-DMAP and, in most cases, the spindle did not rotate. In these eggs, two dense chromatin masses and subsequently, two female pronuclei remained in the egg, usually very close to one another (Fig. 6B, C). In some eggs, a small surface protuberance formed, and then usually disappeared within one hour, although in some cases it remained until the pronuclear stage (Fig. 6C, D). The second polar body was never extruded in oocytes preincubated with 2.5 mM 6-DMAP. Although the polar body did not form, an actin layer was found in the area overlying the spindle and when the spindle did not rotate, or turned slightly, the chromatin was found at a distance from this cortical layer (Fig. 6E). At lower concentrations of 6-DMAP (1.2 mM and 0.6 mM), polar body formation was impaired in most cases.

6-DMAP does not induce the transition to interphase

Since karyokinesis and cytokinesis seemed to be impaired in the presence of 2.5 mM 6-DMAP, we looked at the spindle structure by immunofluorescence using an anti-tubulin antibody in M II-arrested oocytes (Fig. 7A, B). Even after a 3 h treatment with three concentrations of the drug (0.6 mM, 1.2 mM and 2.5 mM), the spindles looked almost normal: we only observed a slight, non significant, decrease in the spindle volume (Fig. 7C) and the presence of some astral microtubules at the spindle poles (Fig. 7B). However, numerous cytoplasmic asters were observed and their number increased when higher doses of the drug were used (Fig. 7B, D). All these effects were clearly dose-dependent. These observations also suggested that the oocytes remained in M-phase despite the presence of 6-DMAP.

This was confirmed when we checked the histone H1 kinase activity in 6-DMAP-treated, M II-arrested oocytes. We found that although 6-DMAP is able to inhibit the mouse H1 kinase activity in our in vitro assay, it did not induce a drop in the kinase activity when oocytes were treated for 3 h with the drug (Fig. 8A). This is in agreement with observation that the metaphase II oocytes stay in M-phase, even during prolonged culture in the presence of 6-DMAP (Rime et al., 1989; Szöllösi et al., 1991).

To follow the effects of 6-DMAP on protein phosphorylation we used two different approaches. The first was to examine the pattern of ^{35}S-methionine-labelled proteins, since it has been shown that the major band shifts observed after fertilization or activation are due to dephosphorylation events (Howlett, 1986). The second was to look directly at the pattern of ^{32}P-phosphate incorporation in oocytes cultured in the presence or absence of 6-DMAP. We did not see any changes in the pattern of newly synthesized proteins after ^{35}S-labelling in M II-arrested oocytes treated for 3 h with 6-DMAP (Fig. 9). However, a decrease in ^{32}P-phosphate incorporation was observed after 3 h of treatment (Fig. 10). This shows that 6-DMAP is able to decrease the turnover of phosphate in M II-arrested oocytes. However, it is not able to inhibit completely phosphate incorporation as some proteins are still phosphorylated.

6-DMAP does not modify the timing of H1 kinase inactivation

6-DMAP did not inhibit either parthenogenetic activation or fertilization, since more than 90% of the oocytes were released from the M II arrest in both cases. We chose artificial activation, which is easy to produce, as a model in which to study the influence of 6-DMAP on histone H1 kinase activity. We found that the activity of histone H1 kinase was not changed in activated oocytes (control and drug-treated) during the first 13-15 min following ethanol treatment (the presumed time of the metaphase-anaphase transition in control activated oocytes). A drop in H1 kinase activity was observed just after this time point in all groups (controls and experimental, preincubated with or without 6-DMAP). These observations suggested that histone H1 kinase activity drops during anaphase II and that both

events are not accelerated by 6-DMAP. In order to verify this hypothesis, we collected at the same time a group of 40 oocytes to measure the histone H1 kinase activity and a group of 20 oocytes that were fixed immediately and stained with Hoechst to assess cytologically the mitotic status of the oocytes during the first 20 min following

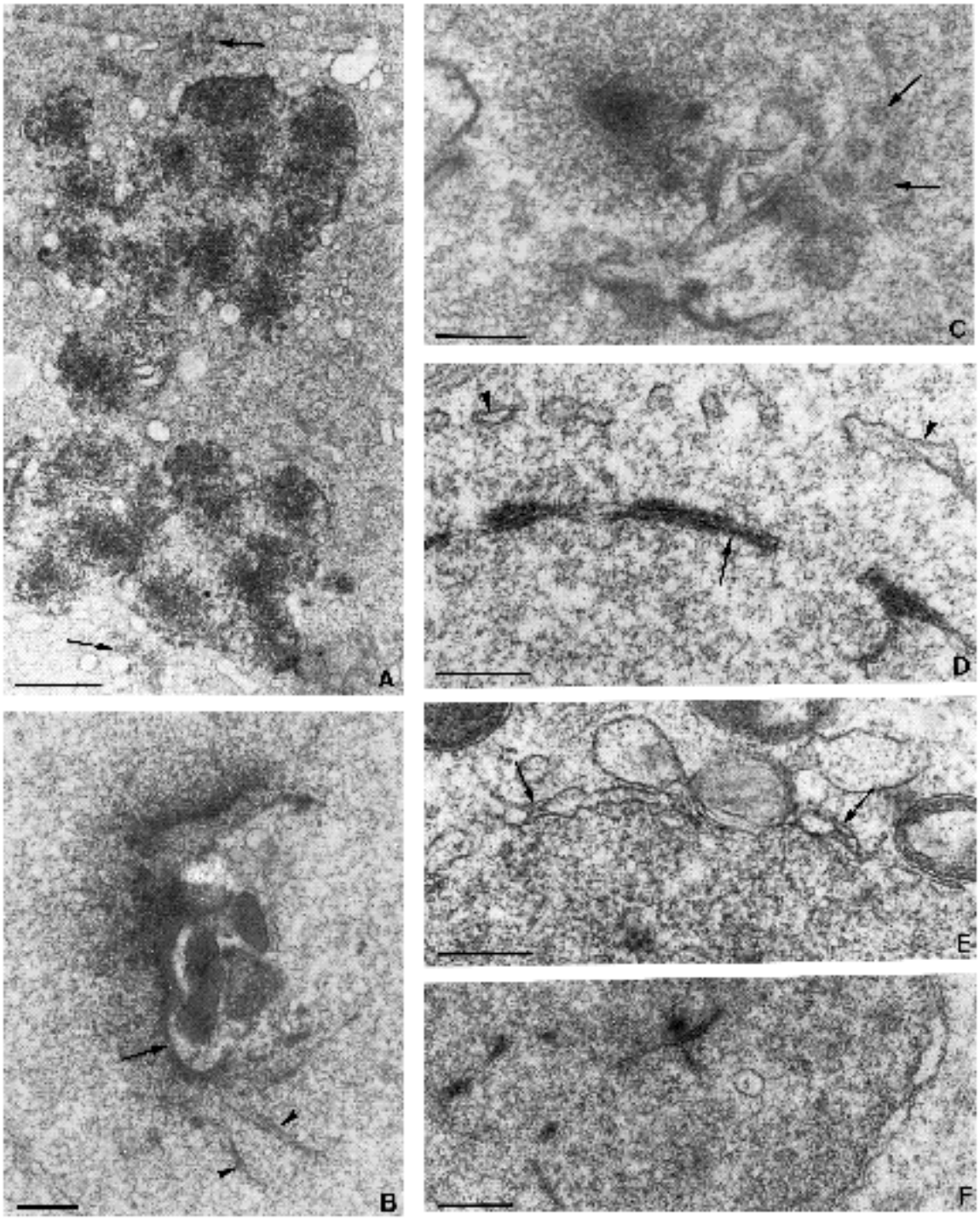

Fig. 5. Ultrastructure of male and female chromatin in oocytes treated with 2.5 mM 6-DMAP. (A) Forming female pronucleus in an activated egg pretreated with 6-DMAP. The arrows point to two microtubule organizing centers (MTOCs). Bar, 1 μm. (B-E) Remodelling sperm chromatin in a fertilized egg treated with 6-DMAP. Bars, 0.25 μm. Note in B, the condensed chromatin in contact with the implantation fossa (arrow) and the presence of chromatin filaments (arrowheads). In C, redundant nuclear envelope containing pores (arrows) of sperm origin are located near the posterior part of the decondensing sperm nucleus. In D, the decondensing sperm chromatin with chromatin filaments (arrows) is surrounded by membrane vesicles originating from the sperm nuclear envelope (arrowheads). In E, note the formation of a new nuclear envelope with pores (arrows) around the recondensing sperm chromatin. (F) Recondensed sperm chromatin surrounded by a nuclear envelope with pores. Note the presence of chromatin filaments. Bar, 0.25 μm.

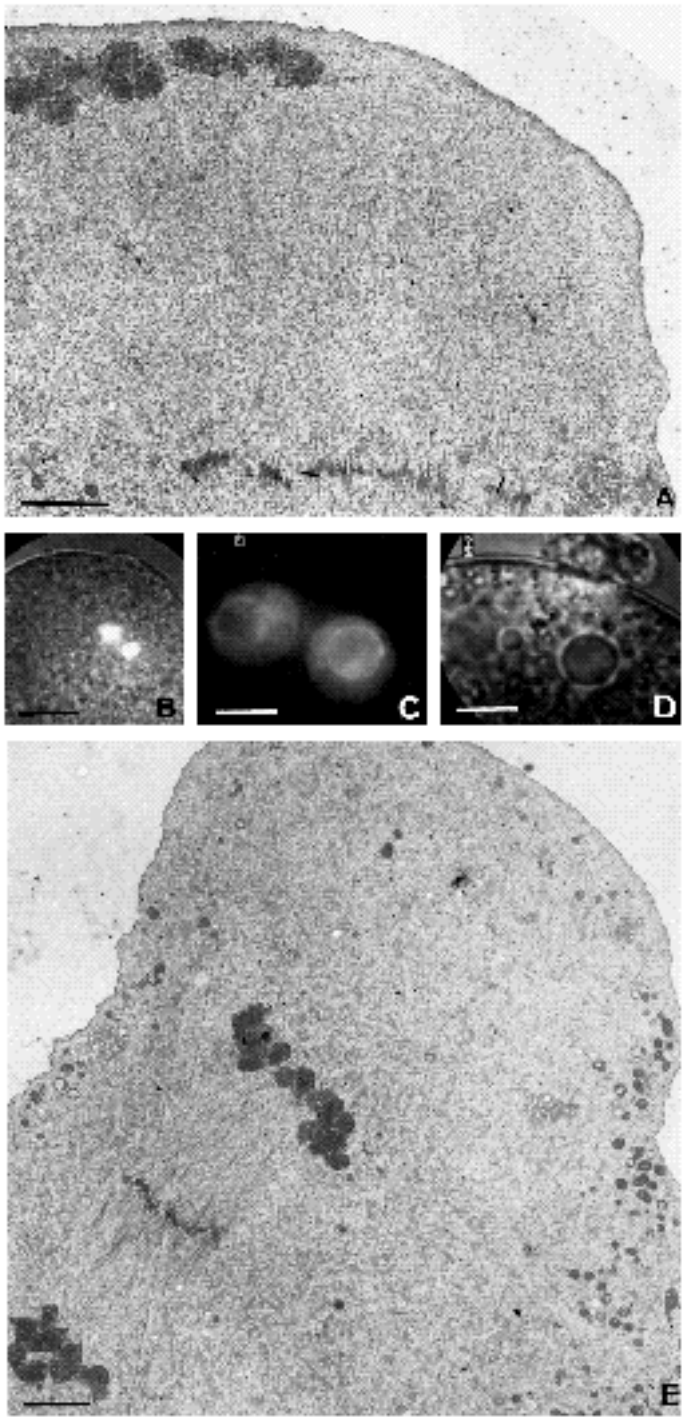

Fig. 6. 6-DMAP inhibits second polar body extrusion. (A) Spindle rotation in a control egg. Note that the chromosomes are located close to the cortical actin layer. Bar, 2 μm. (B) Two dense female chromatin masses in an oocyte activated in the presence of 6-DMAP. Note that the spindle did not rotate and that a small surface protuberance formed. Bar, 10 μm. (C, D) Two nuclei in the cytoplasm of an oocyte activated in the presence of 6-DMAP. Note that the polar body does not contain chromatin. Bar, 10 μm. (E) Partial spindle rotation in an oocyte activated in the presence of 6-DMAP. Note that the chromatin is located at a distance from a cortical microfilament layer. Bar, 2.5 μm.

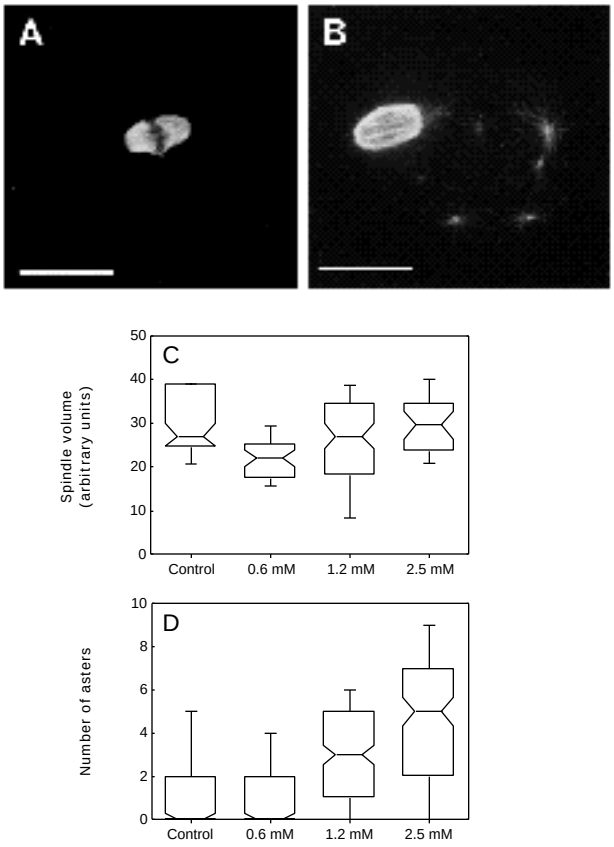

Fig. 7. Effect of 6-DMAP on microtubule organization in M II-arrested oocytes. (A) control metaphase II oocyte stained with an anti-tubulin antibody. (B) metaphase II oocyte treated for 3 h with 2.4 mM 6-DMAP and stained with an anti-tubulin antibody. Note the presence of astral fibers and of cytoplasmic asters. (C) Spindle volume (in arbitrary units) in control and 6-DMAP treated (0.6 mM, 1.2 mM and 2.5 mM for 3 h) metaphase II oocytes. (D) Number of asters in control and 6-DMAP treated (0.6 mM, 1.2 mM and 2.5 mM for 3 h) metaphase II oocytes. The box plots display the 10th, 25th, 50th, 75th and 90th percentiles for each group. The number of oocytes scored were 62 (control), 41 (0.6 mM), 76 (1.2 mM) and 30 (2.5 mM) to measure the spindle volume (C) and 150 (control), 144 (0.6 mM), 220 (1.2 mM) and 137 (2.5 mM) to count the number of cytoplasmic asters (D).

ethanol treatment. The results shown in Fig. 8B confirmed that the drop of histone H1 kinase activity takes place at anaphase II, and that 6-DMAP does not interfere with the timing of both processes.

6-DMAP inhibits protein phosphorylation in activated eggs

When ^{35}S-methionine-labelled proteins were observed in control eggs, we confirmed the observations of Howlett (1986). The newly synthesized 35 kDa complex was still phosphorylated 3 h after activation (upper and middle bands still present), whilst the newly synthesized 30 kDa polypeptide was not phosphorylated 1 h after activation (lower band present; Fig. 9). The chase experiments showed that the 35 kDa complex phosphorylated in M-phase was not dephosphorylated, whereas the 30 kDa protein was slowly dephosphorylated during this 3 h period (Fig. 9).

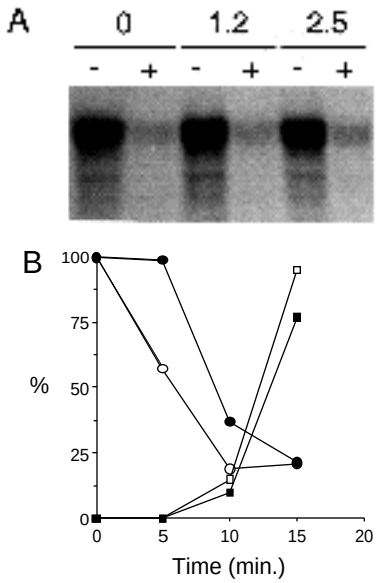

Fig. 8. (A) Histone kinase activity in metaphase II oocytes treated for 3 h with 6-DMAP; 0, control; 1.2, 1.2 mM; 2.5, 2.5 mM 6-DMAP. (B) Activated oocytes in the absence (○ □) or presence (● ■) of 2.5 mM 6-DMAP. Percentage of residual histone kinase activity (○ ●) and percentage of anaphase II (□ ■) in the cultures at various time points after activation.

In the presence of 6-DMAP, the phosphorylation of the newly synthesized 35 kDa polypeptides was progressively inhibited and the dephosphorylation of the 30 kDa protein and 35 kDa complex was accelerated.

^{32}P-labelling allowed us to show that 6-DMAP inhibited the phosphorylation of the major phosphoprotein bands, the 35 kDa complex and a band at around 71 kDa, and accelerated their dephosphorylation in activated oocytes (Fig. 10).

DISCUSSION

After fertilization (or activation) of the mouse oocyte, a very distinctive period takes place during the transition between meiosis and the first mitotic interphase. After the completion of karyokinesis, the chromosomes remain condensed without formation of a nuclear envelope and the interphase network of microtubules is not formed. It is only at the dense chromatin mass stage (see Results) that the nuclear envelope forms and that the cytoplasmic network of microtubules appears. The major finding described in this paper is that this transition can be accelerated by the kinase inhibitor 6-DMAP.

6-DMAP and kinase inhibition

We show that there is a differential effect of 6-DMAP between M II-arrested and activated oocytes. 6-DMAP clearly inhibits in vitro histone H1 kinase in M II oocyte extracts. However, extracts made from 6-DMAP-treated M II-arrested oocytes still retain a full level of histone H1 kinase activity (when 6-DMAP has not been added into the reaction tube). This suggests that 6-DMAP is not able to induce MPF destruction in vivo in M II-arrested oocytes. It is possible that 6-DMAP does not enter the metaphase oocytes, but we observed that the drug induced (1) the formation of microtubule asters; (2) a decrease in phosphate incorporation in the 35 kDa and 71 kDa phosphoproteins

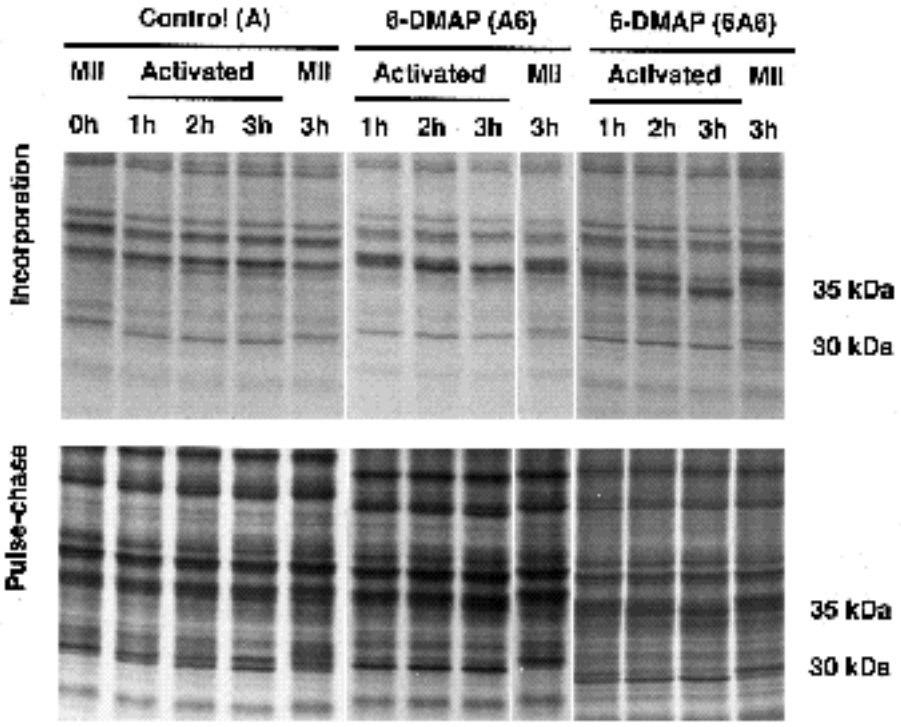

Fig. 9. Patterns of ^{35}S-methionine-labelled proteins in activated oocytes cultured in the absence or presence of 2.5 mM 6-DMAP. Top panels: eggs were labelled for 1 h at the time indicated. Bottom panel: oocytes were labelled for 1 h at the metaphase II (MII) stage and chased in cold methionine. Metaphase II oocytes and activated eggs were recovered at the time indicated.

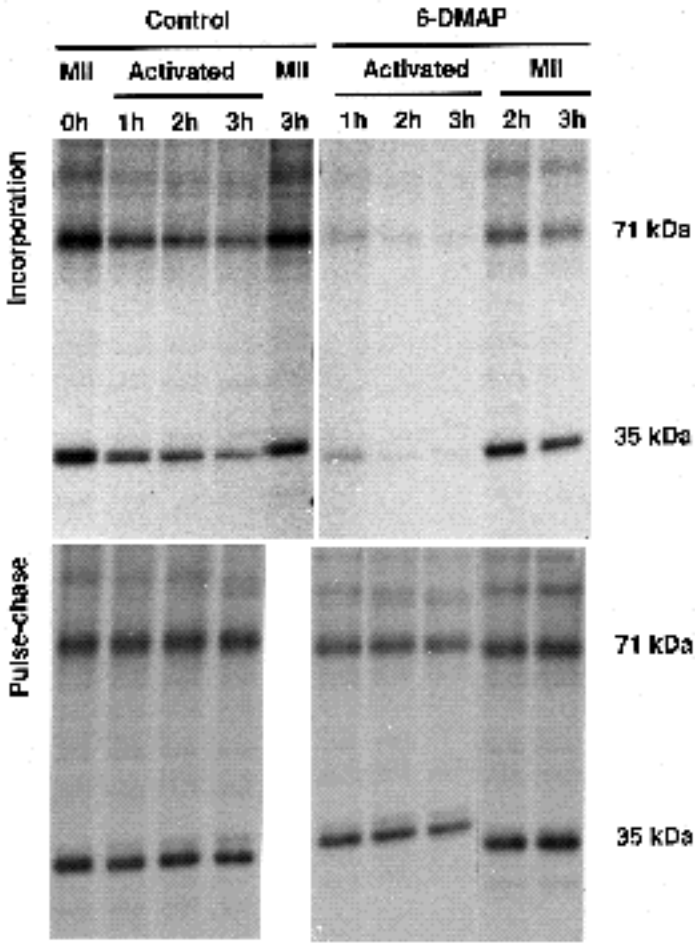

Fig. 10. Patterns of ^{32}P-phosphate-labelled proteins in activated oocytes cultured in the absence or presence of 2.5 mM 6-DMAP. Top panels: eggs were labelled for 1 h at the time indicated. Bottom panel: oocytes were labelled for 1 hr at the metaphase II stage and chased in cold phosphate. Metaphase II oocytes and activated eggs were recovered at the time indicated.

and (3) a further acceleration of the transition to interphase in oocytes that had been preincubated with the drug before activation. These observations strongly suggest that 6-DMAP enters M II-arrested oocytes; however, we cannot exclude that the penetration of the drug is lower in M II when compared to the transitional period. It might be expected that inhibition of kinase enzymes by 6-DMAP during M-phase, when their activity is normally high (Howlett and Bolton, 1985; Karsenti et al., 1987), would lead to the dephosphorylation of numerous proteins (since the activity of protein phosphatases should remain unchanged) and consequently, induce the transition to interphase. However, to our knowledge, there are no reports showing that 6-DMAP induces this transition, when added to metaphase cell-free extracts. In addition, there is no evidence to show that inhibition of the cdc2 kinase by 6-DMAP in M-phase extracts induces cyclin destruction and thus MPF inactivation. On the contrary, the cdc2 kinase itself has been shown to trigger cyclin degradation in interphase extracts of amphibian eggs (Félix et al., 1990). 6-DMAP only inhibited changes in microtubule dynamics, when added together with active cdc2 kinase to interphase extracts (Verde et al., 1990, 1991). We observed the formation of asters in M II-arrested oocytes, suggesting that 6-DMAP stabilizes microtubules in the oocyte, as expected from the in vitro experiments. We must also point out that mouse oocytes incubated with 6-DMAP just after germinal vesicle breakdown form interphase nuclei within 7 h, whereas the application of 6-DMAP just after the metaphase I/anaphase I transition leads to the formation of nuclei within 1.5 h of culture (Szöllösi et al., 1991; Szöllösi and Debey, unpublished data). Taken together, these data suggest that 6-DMAP can only induce the formation of interphase nuclei once the MPF fall has been triggered independently from 6-DMAP action.

After oocyte activation, the inhibitory effect of 6-DMAP on kinase activity leads to a dramatic acceleration of the transition between the second meiotic M-phase and the first mitotic interphase. This is correlated with modifications in the pattern of phosphorylation of a 35 kDa protein complex. This complex is phosphorylated during the metaphase II arrest and slowly dephosphorylated after activation, although phosphorylation of the newly synthesized 35 kDa proteins is still observed during the first few hours after oocyte activation (Howlett, 1986; Howlett and Bolton, 1985). Our results show that 6-DMAP inhibits this phosphorylation, probably by inhibiting directly the corresponding kinase(s).

6-DMAP and polar body formation

6-DMAP inhibits spindle rotation and second polar body formation. These two events are controlled by interactions between the chromosomes and the oocyte cortex, resulting in the formation of a microfilament-rich domain overlying the spindle (Maro et al., 1986). During normal activation, a close association between one of the rotating spindle poles and the cortical actin layer can be observed. The lack of this contact in the presence of 6-DMAP suggests that protein phosphorylation is involved in the maintenance of the spindle pole-cortex association and successful spindle rotation. Extrusion of the first polar body was also often inhibited by this drug during mouse oocyte maturation (Szöllösi et al., 1991), as well as the formation of both polar bodies in maturing oocytes of Echinoderms (Néant et al., 1989). 6-DMAP does not visibly change actin organization. The thick microfilament layer overlying the M II spindle persists and a thick layer of microfilaments forms over the decondensing sperm in the presence of the drug, as during normal fertilization (Karasiewicz and Sołtyńska, 1985; Maro et al., 1984). Cytochalasin D, a microfilament inhibitor, prevents the extrusion of the second polar body and the formation of the incorporation cone (Maro et al., 1984), as does 6-DMAP. This suggests that 6-DMAP inhibits contractile activity in the cortex after activation. This may be linked to the absence of phosphorylation at the activating phosphorylation site of the myosin II regulatory light chain at telophase, thus decreasing contractile activity in the furrow (Satterwhite et al., 1989; Satterwhite and Pollard, 1992). In addition, 6-DMAP changes the outline of the cell surface in mature and activated eggs, causing it to become folded very irregularly, like in maturing

oocytes (Szöllösi et al., 1991), suggesting an uncontrolled cortical activity.

6-DMAP and microtubules

In metaphase II-arrested oocytes, 6-DMAP modifies slightly the organization of the microtubule network. Astral microtubules can be observed at the spindle poles and cytoplasmic asters are present, suggesting that the drug facilitates microtubule polymerization in the oocyte. This is consistent with the observations of Verde et al. (1990) in *Xenopus* egg extracts, where 6-DMAP was used to inhibit the $p34^{cdc2}$ kinase and was able to block the shrinking of microtubules induced by the $p34^{cdc2}$ kinase. In control, activated mouse eggs, the interphase network of microtubules does not form until 1 h after the beginning of the second polar body extrusion. During this period, the microtubules behave as if they were still in M-phase, despite the drop in H1 kinase activity (Weber, Kubiak and Maro, unpublished). 6-DMAP accelerates the formation of the interphase network, suggesting that it inhibits a kinase involved in the regulation of the microtubule network, such as the MAP kinase. It has been shown that this serine-threonine kinase is able to induce the interphase-metaphase transition of the microtubule network in interphase extracts from *Xenopus* eggs (Gotoh et al., 1991). The observed behaviour of microtubules in 6-DMAP-treated, M II-arrested oocytes and activated eggs is consistent with an inhibitory effect of the drug on MAP kinase.

6-DMAP and the formation of pronuclei

6-DMAP accelerates the formation of both pronuclei. Nuclear envelope assembly around the female chromatin takes place very rapidly, sometimes even before the formation of clear telophase masses. However, after fertilization, 6-DMAP interferes with the remodelling of the sperm nucleus into a male pronucleus. The nuclear envelope breaks down in small vesicles, but these are not dispersed in the cytoplasm and stay around the decondensing chromatin. Mouse sperm nuclei contain protamines but lack somatic histones and transition proteins (Pogany et al., 1981). Chromatin decondensation proceeds first by reduction of the sperm nuclear disulfide bonds, and then by destabilization of the DNA/protamine complex, probably as a result of protamine phosphorylation (Wiesel and Schultz, 1981) that may be due to the protein kinase C (Nishiyama et al., 1988). Chromatin recondensation is accelerated in the presence of 6-DMAP. However, the bundles of chromatin filaments present at the beginning of the decondensation period disappear rapidly in controls but remain for a long time in the presence of the drug. They are even found in the recondensed sperm chromatin after formation of a new nuclear envelope. The last part of the sperm chromatin to decondense in presence of 6-DMAP is the posterior part, perhaps due to the link that exists between the chromatin and the nuclear annulus (Ward and Coffey, 1989). This is also the area of chromatin that condenses last during spermatogenesis (Czaker, 1987). It was still condensed when the rest of the chromatin was already decondensed and had started the transitional recondensation. These two anomalies suggest that 6-DMAP might perturb the exchange of the DNA-associated proteins. We will test this hypothesis by studying the presence of protamine and histone by immunofluorescence during the sperm nuclear remodelling in the presence of the drug.

The remodelling of the sperm nucleus was also accelerated in oocyte fragments penetrated in vitro 3 h after parthenogenetic activation (Borsuk, 1991; Borsuk and Tarkowski, 1989; Szöllösi, Borsuk and Szöllösi, unpublished). This coincides with the normal period of dephosphorylation of the 35 kDa protein complex (Howlett and Bolton, 1985; this paper). These data support a possible role of this protein complex in the transformation of the sperm head into a pronucleus after fertilization. If the dephosphorylation of these proteins is involved in the regulation of the dynamics of sperm nucleus remodelling in the oocyte, their slow dephosphorylation during normal fertilization might prevent a too rapid remodelling of the sperm nucleus, that may lead to abnormalities (as it is the case in the presence of 6-DMAP). It seems clear that the kinase(s) implicated in the phosphorylation of the 35 kDa complex is (are) inhibited by 6-DMAP, but only after MPF inactivation. Thus, it is tempting to speculate that two different subpopulations of kinases able to phosphorylate the 35 kDa complex are active during M-phase and after activation, some of those active during the M II arrest being insensitive to 6-DMAP.

In conclusion, our data show that 6-DMAP inhibits some unidentified kinases, and accelerates some post-fertilization events in mouse oocytes. Inhibition of these kinases does not have an impact on MPF activity during the M II arrest, or on the dynamics of MPF inactivation during oocyte activation. Some of these 6-DMAP-sensitive kinases are involved in the regulation of the polymerization of microtubules, nuclear envelope assembly and chromatin remodelling.

We are grateful to Dr N. Winston for critical reading of the manuscript, Ms D. Huneau for providing high quality thin sections for the electron microscope study and to R. Scandolo, R. Schwartzmann and J. Hamel for their expert photographic work. Part of this work was supported by grants from the Institut National pour la Santé et la Recherche Medicale, the Ligue Nationale contre le Cancer, the Association pour la Recherche contre le Cancer and the Fondation pour la Recherche Médicale (FRM) to Bernard Maro and the FRM to Pascale Debey. Jacek Kubiak is the recipient of a fellowship from the FRM and Henri de Pennart from the Ligue Nationale contre le Cancer.

REFERENCES

Adenot, P. G., Szöllösi, M. S., Geze, M., Renard, J. P. and Debey, P. (1991). Dynamics of paternal chromatin changes in live one-cell mouse embryos after natural fertilization. *Mol. Reprod. Dev.* **28**, 23-34.

Borsuk, E. (1991). Anucleate fragments of parthenogenetic eggs and of maturing oocytes contain complementary factors required for development of a male pronucleus. *Mol. Reprod. Dev.* **29,** 150-156.

Borsuk, E. and Tarkowski, A. K. (1989). Transformation of sperm nuclei into male pronuclei in nucleate and anucleate fragments of parthenogenetic mouse eggs. *Gamete Res.* **24,** 471-481.

Choi, T., Aoki, F., Mori, M., Yamashita, M., Nagahama, Y. and Kohmoto, K. (1991). Activation of $p34^{cdc2}$ protein kinase activity in meiotic and mitotic cell cycles in mouse oocytes and embryos. *Development* **113,** 789-795.

Cuthberson, K. S. R. (1983). Parthenogenetic activation of mouse oocytes in vitro with ethanol and benzyl alcohol. *J. Exp. Zool.* **226,** 311-314.

Czaker, R. (1987). Relative position of constitutive heterochromatin and of nucleolar structure during mouse spermiogenesis. *Anat. Embryol.* **175,** 467-475.

de Pennart, H., Houliston, E. and Maro, B. (1988). Post-translational modifications of tubulin and the dynamics of microtubules in mouse oocytes and zygotes. *Biol. Cell* **64,** 375-378.

Debey, P., Renard, J.-P., Coppey-Moisan, M., Monnot, I. and Geze, M. (1989). Dynamics of chromatin changes in live one-cell mouse embryos: a continuous follow-up by fluorescence microscopy. *Exp. Cell Res.* **183,** 413-433.

Félix, M. A., Labbe, J. C., Dorée, M., Hunt, T. and Karsenti, E. (1990). Triggering of cyclin degradation in interphase extracts of amphibian eggs by cdc2 kinase. *Nature* **346,** 379-382.

Félix, M. A., Pines, J., Hunt, T. and Karsenti, E. (1989). A post-ribosomal supernatant from activated Xenopus eggs that displays post-translationally regulated oscillation of its cdc2+ mitotic kinase activity. *EMBO J.* **8,** 3059-3069.

Fraser, L. R. and Drury, L. (1975). The relationship between sperm concentration and fertilisation in vitro of mouse eggs. *Biol. Reprod.* **13,** 513-518.

Gotoh, Y., Nishida, E., Matsuda, S., Shiina, N., Kosako, H., Shiokawa, K., Akiyama, T., Ohta, K. and Sakai, H. (1991). In vitro effects on microtubule dynamics of purified Xenopus M phase-activated MAP kinase. *Nature* **349,** 251-254.

Howlett, S. K. (1986). A set of proteins showing cell cycle-dependent modification in the early mouse embryo. *Cell* **45,** 387-396.

Howlett, S. K. and Bolton, V. N. (1985). Sequence and regulation of morphological and molecular events during the first cell cycle of mouse embryogenesis. *J. Embryol. Exp. Morph.* **87,** 175-206.

Karasiewicz, J. and Sołtyńska, M. S. (1985). Ultrastructural evidence for the presence of actin filaments in mouse eggs at fertilization. *Roux Arch. Dev. Biol.* **194,** 369-372.

Karsenti, E., Bravo, R. and Kirshner, M. (1987). Phosphorylation changes associated with the early cell cycle in *Xenopus* oocytes. *Dev. Biol.* **119,** 442-453.

Kilmartin, J. V., Wright, B. and Milstein, C. (1982). Rat monoclonal antitubulin antibodies derived by using a new nonsecreting rat cell line. *J. Cell Biol.* **93,** 576-582.

Kopečný, V. and Pavlok, A. (1975a). Autoradiographic study of mouse spermatozoan arginine-rich nuclear protein in fertilization. *J. Exp. Zool.* **191,** 85-96.

Kopečný, V. and Pavlok, A. (1975b). Incorporation of arginine-^{3}H into chromatin of mouse eggs shortly after sperm penetration. *Histochemistry* **45,** 341-345.

Kubiak, J. Z., Paldi, A., Weber, M. and Maro, B. (1991). Genetically identical parthenogenetic mouse embryos produced by inhibition of the first meiotic division by cytochalasin D. *Development* **111,** 763-770.

Laemmli, U. K. (1970). Cleavage of structural proteins during the assembly of the head of bacteriophage T4. *Nature* **227,** 11713-11720.

Maro, B., Johnson, M. H., Pickering, S. J. and Flach, G. (1984). Changes in the actin distribution during fertilization of the mouse egg. *J. Embryol. exp. Morph.* **81,** 211-237.

Maro, B., Johnson, M. H., Webb, M. and Flach, G. (1986). Mechanism of polar body formation in the mouse oocyte: an interaction between the chromosomes, the cytoskeleton and the plasma membrane. *J. Embryol. exp. Morph.* **92,** 11-32.

Néant, I., Charbonneau, M. and Guerrier, P. (1989). A requirement for protein phosphorylation in regulating the meiotic and mitotic cell cycles in echinoderms. *Dev. Biol.* **132,** 304-314.

Néant, I. and Guerrier, P. (1988). Meiosis reinitiation in the mollusc *Patella vulgata.* Regulation of MPF, CSF and chromosome condensation activity by intracellular pH, protein synthesis and phosphorylation. *Development* **102,** 505-516.

Nicolson, G. L., Yanagimachi, R. and Yanagimachi, H. (1975). Ultrastructural localization of lectin binding sites on the zonae pellucidae and plasma membranes of mammalian eggs. *J. Cell Biol.* **66,** 263-274.

Nishiyama, K., Sakai, K., Tanaka, Y., Kobayashi, T., Nakamura, S., Sakanoue, Y., Hashimoto, E. and Yamamura, H. (1988). Comparison of phosphorylation sites in protamines between protein kinase C and cAMP-dependent protein kinase. *Biochem. Int.* **17,** 51-58.

Nonchev, S. and Tsanev, R. (1990). Protamine-histone replacement and DNA replication in the male mouse pronucleus. *Mol. Reprod. Develop.* **25,** 72-76.

Pogany, G. C., Corzett, M., Weston, S. and Balhorn, R. (1981). DNA and protein content of mouse sperm. *Exp. Cell Res.* **136,** 127-136.

Quinn, P., Barros, C. and Whittingham, D. G. (1982). Preservation of hamster oocytes to assay the fertilizing capacity of human spermatozoa. *J. Reprod. Fertil.* **66,** 161-168.

Rime, H., Néant, I., Guerrier, P. and Ozon, R. (1989). 6-Dimethylaminopurine (6-DMAP), a reversible inhibitor of the transition to metaphase during the first meiotic cell division of the mouse oocyte. *Dev. Biol.* **133,** 169-179.

Rodman, T. C., Pruslin, F. H., Hoffman, H. P. and Allfrey, V. G. (1981). Turnover of basic chromosomal proteins in fertilized eggs: a cytoimmunochemical study of events in vivo. *J. Cell Biol.* **90,** 351-361.

Satterwhite, L., Cisek, L., Corden, J. and Pollard, T. (1989). A p34cdc2 containing kinase phosphorylates myosin regulatory light chain. *J. Cell Biol.* **109,** 284a.

Satterwhite, L. L. and Pollard, T. D. (1992). Cytokinesis. *Current Opinion in Cell Biology* **4,** 43-52.

Szöllösi, M. S., Debey, P., Szöllösi, D., Rime, H. and Vautier, D. (1991). Chromatin behaviour under the influence of puromycin and 6-DMAP at different stages of mouse oocyte maturation. *Chromosoma* **100,** 339-354.

Verde, F., Berrez, J. M., Antony, C. and Karsenti, E. (1991). Taxol-induced microtubule asters in mitotic extracts of *Xenopus* eggs - requirement for phosphorylated factors and cytoplasmic dynein. *J. Cell Biol.* **112,** 1177-1187.

Verde, F., Labbé, J.-C., Dorée, M. and Karsenti, E. (1990). Regulation of microtubule dynamics by cdc2 prote^{o}ßin kinase in cell-free extracts of Xenopus eggs. *Nature* **343,** 233-238.

Ward, W. S. and Coffey, D. S. (1989). Identification of a sperm nuclear annulus: a sperm DNA anchor. *Biol. Reprod.* **41,** 361-370.

Weber, M., Kubiak, J. Z., Arlinghaus, R. B., Pines, J. and Maro, B. (1991). *c-mos* proto-oncogene product is partly degraded after release from meiotic arrest and persists during interphase in mouse zygotes. *Dev. Biol.* **148,** 393-397.

Wiesel, S. and Schultz, G. A. (1981). Factors which may affect removal of protamine from sperm DNA during fertilization in the rabbit. *Gamete Res.* **4,** 25-34.

Witkowska, A. (1981). Pronuclear development and the first cleavage division in polyspermic mouse eggs. *J. Reprod. Fert.* **62,** 493-498.

Yotsuyanagi, Y. and Szöllösi, D. (1981). Early mouse embryo intracisternal particle: fourth type of retrovirus-like particles associated with the mouse. *J. Nat. Cancer Inst.* **67,** 677-685.

(Received 8 July 1992 - Accepted, in revised form, 8 December 1992)